

Cost-Effective Surface-Mounted Patch Antenna with Ring Slot Using Ball Grid Array Packaging for 5G Millimeter-Wave Applications

Xiubo Liu¹, Wei Zhang¹, Dongning Hao¹, and Yanyan Liu^{2, *}

Abstract—The letter presents a compact, cost-effective, and surface-mount patch antenna element for 5G millimeter-wave (mmWave) system integration. The antenna element adopts ball grid array (BGA) packaging technology to achieve surface mount function, which can be applied to highly integrated systems. By adding a ring slot on the radiating patch, the proposed antenna obtains a wider impedance bandwidth. The antenna prototype has been simulated, manufactured, and verified. The proposed antenna element size is $5\text{ mm} \times 5\text{ mm} \times 1.3\text{ mm}$. The measurement results show that the proposed antenna element can be used in the N257 (26.5 to 29.5 GHz) and N261 (27.5–28.35 GHz) frequency bands.

1. INTRODUCTION

The concept of microstrip patch antenna has been studied since 1960 [1]. Due to its compact size, easy manufacture, and low cost, it is very suitable for use in many applications. The disadvantage of the microstrip antenna is its narrow bandwidth. Many studies have been carried out to increase the bandwidth of a microstrip antenna. For example, stacked configuration is proposed to increase the bandwidth of the microstrip patch antenna [2], and the ultrawideband impedance of semicircular patch with semicircular slots is 146.67% [3]. Furthermore, loading U-slot on a patch is one of the most popular methods to increase bandwidth [4–7]. However, bulky coaxial cables are a major challenge for RF system integration, especially in the mmWave frequency band.

Antenna-in-Package (AiP) is a packaging technology that integrates active chipsets and antennas in the standard surface-mount device to achieve high integration [8–11]. Ball grid array packaging is a standard packaging technology that can achieve low cost, high performance, and automatic assembly [12–14]. On the other hand, the cost is one of the main challenges for 5G millimeter-wave antennas due to the high loss of high-frequency band. Recently, many cost-effective antennas have been reported [15–19]. FR4 substrate can be seen as an effective way to reduce costs. Single-layer FR4 substrates further reduce costs, such as planar inverted F antennas (PIFA) [18] and U-shaped slot patch antennas [19]. In this letter, a BGA packaged patch antenna with a ring slot for 5G mmWave system integration is introduced. An FR4 printed circuit board is used as the substrate to meet cost-effective requirements. The design process is introduced in detail. The antenna prototype has been manufactured and measured for verification. All simulation results are given by ANSYS HFSS.

2. ANTENNA GEOMETRY AND DESIGN

Figure 1 shows the structure of the proposed antenna element. The antenna is manufactured using a standard printed circuit board (PCB) technology. The relative permittivity of the FR4 substrate is

Received 1 July 2021, Accepted 9 August 2021, Scheduled 16 August 2021

* Corresponding author: Yanyan Liu (lyytianjin@nankai.edu.cn).

¹ School of Microelectronics, Tianjin University, Tianjin 300072, China. ² Tianjin Key Laboratory of Photo-electronic Thin Film Devices and Technology, Nankai University, Tianjin 300071, China.

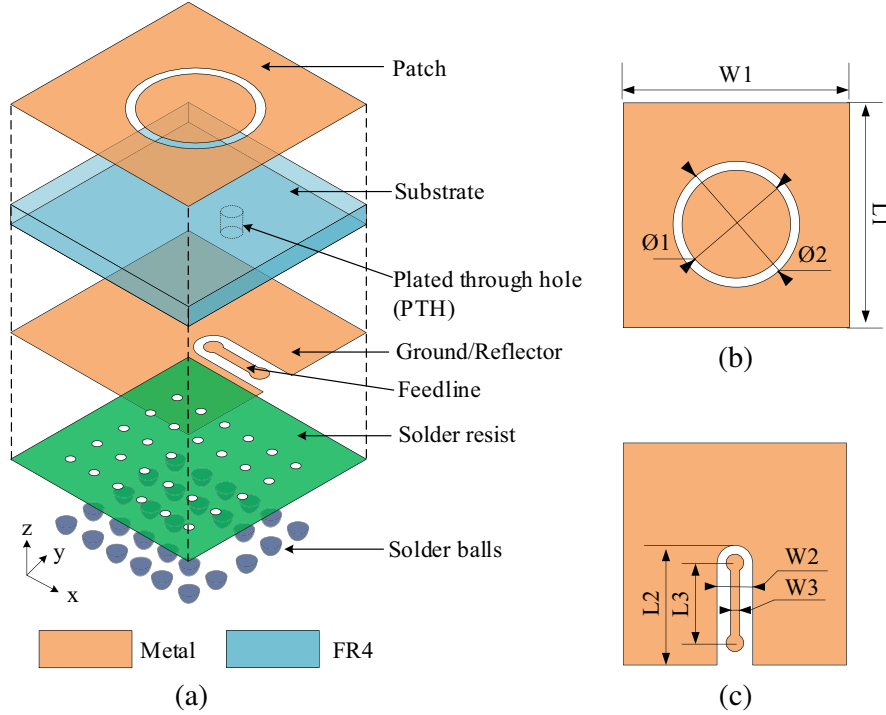


Figure 1. Geometry of the proposed antenna element. (a) Exploded view. (b) Top view. (c) Bottom view. ($L1 = 5$, $L2 = 2.7$, $L3 = 1.8$, $W1 = 5$, $W2 = 0.8$, $W3 = 0.2$, $\Phi1 = 2.4$, $\Phi2 = 2.8$, Units: mm).

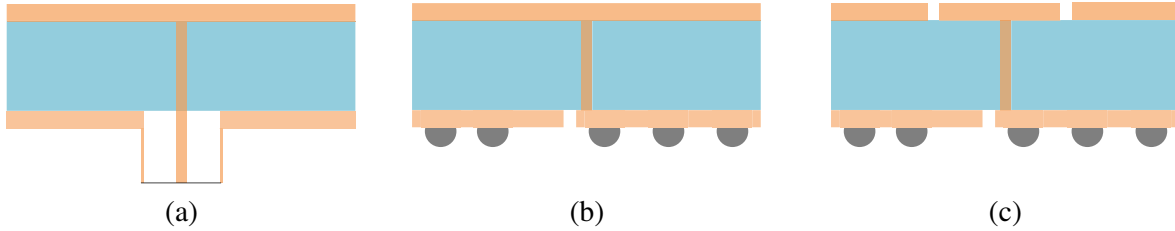


Figure 2. Evolution of the proposed antenna. (a) Coaxial cable fed patch antenna. (b) BGA packaged patch antenna without ring slot. (c) BGA packaged patch antenna with ring slot.

4.4; the dielectric loss tangent is 0.018; and the thickness is 1.1 mm. The antenna element includes a dielectric layer, a solder resists layer, and two metal layers. The patch and ring slot are etched on the top metal layer. The ground plane and feedline are made on the bottom metal layer. In addition, the feedline and patch are connected through plated through holes (PTH). Finally, the solder balls with a diameter of $300\ \mu\text{m}$ are mounted on the bottom layer to complete the BGA packaging. To facilitate the interconnection with the RF chipset, the input impedance of the antenna element is set to be $50\ \Omega$.

The evolution of the proposed antenna is shown in Figure 2. Figure 2(a) shows a conventional patch antenna fed by a coaxial cable. However, coaxial cables are difficult to integrate into RF systems. Figure 2(b) shows the BGA packaged patch antenna, which can be surface mounted and easily integrated into the RF system without bulky coaxial cables. In addition, Figure 2(c) adds a ring slot to the prototype of Figure 2(b). It can be seen that the ring slot increases the bandwidth and maintains the same compact size.

Figures 3(a) and (b) show the simulated surface current distribution at 30 GHz. As shown in Figure 3(a), when there is no ring slot on the patch, the patch is excited by the PTH, the surface current is concentrated on the edge. When the ring slot is added to the patch, as shown in Figure 3(b), the surface current is distributed on the circular edge and coupled to the patch. Figure 3(c) shows the

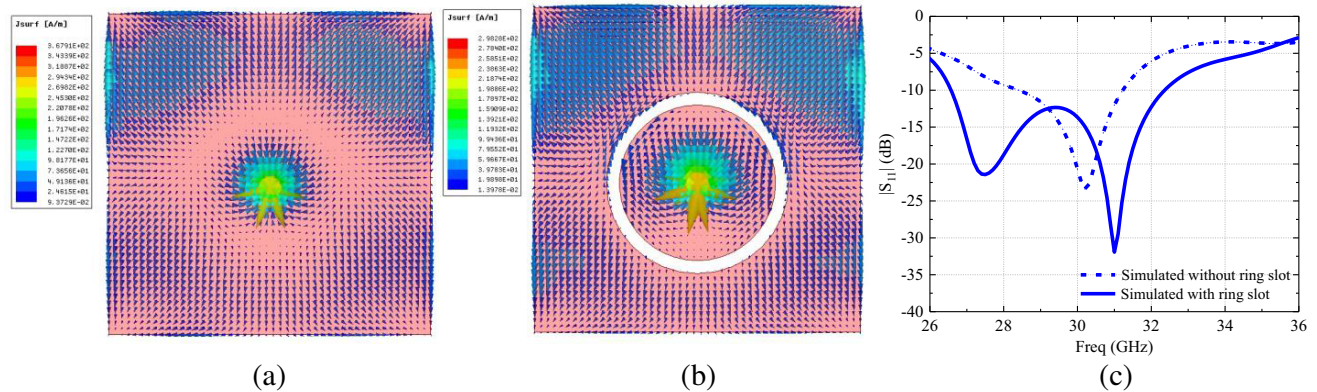


Figure 3. Simulated surface current distribution at 30 GHz. (a) Without ring slot. (b) With ring slot. (c) Simulated reflection coefficient of the proposed antenna with/without the ring slot.

reflection coefficient of the proposed antenna. The simulated impedance of -10 dB ranges from 28.5 to 31.2 GHz for the design without the ring slot. Besides, the design with the ring slot shows -10 dB impedance bandwidth ranging from 26.6 to 32.3 GHz. It can be seen that the bandwidth of the antenna with a ring slot is much wider than the antenna without a ring slot. Most importantly, the antenna maintains the same size at the same time.

3. MEASUREMENT RESULTS AND DISCUSSION

Figure 4 shows a photograph of the manufactured prototype. Figure 4(a) shows the top and bottom views of the proposed antenna element. Figure 4(b) shows the assembled prototype. The antenna element is mounted on a RO4350B evaluation board with a relative permittivity of 3.66, a dielectric loss tangent of 0.0037, and a thickness of 0.254 mm. In addition, the 50Ω grounded coplanar waveguide (GCPW) feedline is designed on the evaluation board (14 mm \times 13 mm) with a width of 0.54 mm, and a gap of 0.43 mm. A 2.92 mm end launch connector is installed at the end of the evaluation board to connect the measurement coaxial cable. The reflection coefficient is measured by Rohde & Schwarz Network Analyzer (ZVA40), and the radiation patterns are measured in a standard anechoic chamber.

3.1. Measured Results

Figure 4(c) shows the simulated and measured reflection coefficients. It can be seen that the simulated impedance bandwidth of -10 dB is from 26.6 to 32.3 GHz. The measured reflection coefficient deteriorates at 30.4 GHz, so we give a measured bandwidth of -9.94 dB. It can be observed that the measured impedance bandwidth of -9.94 dB ranges from 26.6 to 35.7 GHz. Figure 4(d) shows the simulated and measured peak gains of the antenna. The proposed antenna element focuses on the N257 and N261 frequency bands, so we only give the antenna gain of 27–32 GHz. The simulated gain is 2.98 to 5.53 dBi, and the measured gain is 1.87 to 5.2 dBi. Besides, the simulated efficiency is above 69.5% in the range of 27–32 GHz. The discrepancy is mainly caused by manufacturing tolerances. The processing tolerance has a great influence on the performance of the antenna, especially in the mmWave frequency band. Figure 6 shows the simulated and measured E -plane and H -plane normalized radiation patterns at 28 GHz, 30 GHz, and 32 GHz. It can be observed that an acceptable agreement is obtained between the simulated and measured results.

3.2. Tolerance Analysis

Manufacturing accuracy is the main factor affecting the performance of millimeter-wave antennas. As shown in Figure 4(c), there is a deviation between the simulation and measurement results. In general, the PCB substrate size is slightly wider than the metal layer. This part is a challenge for very small

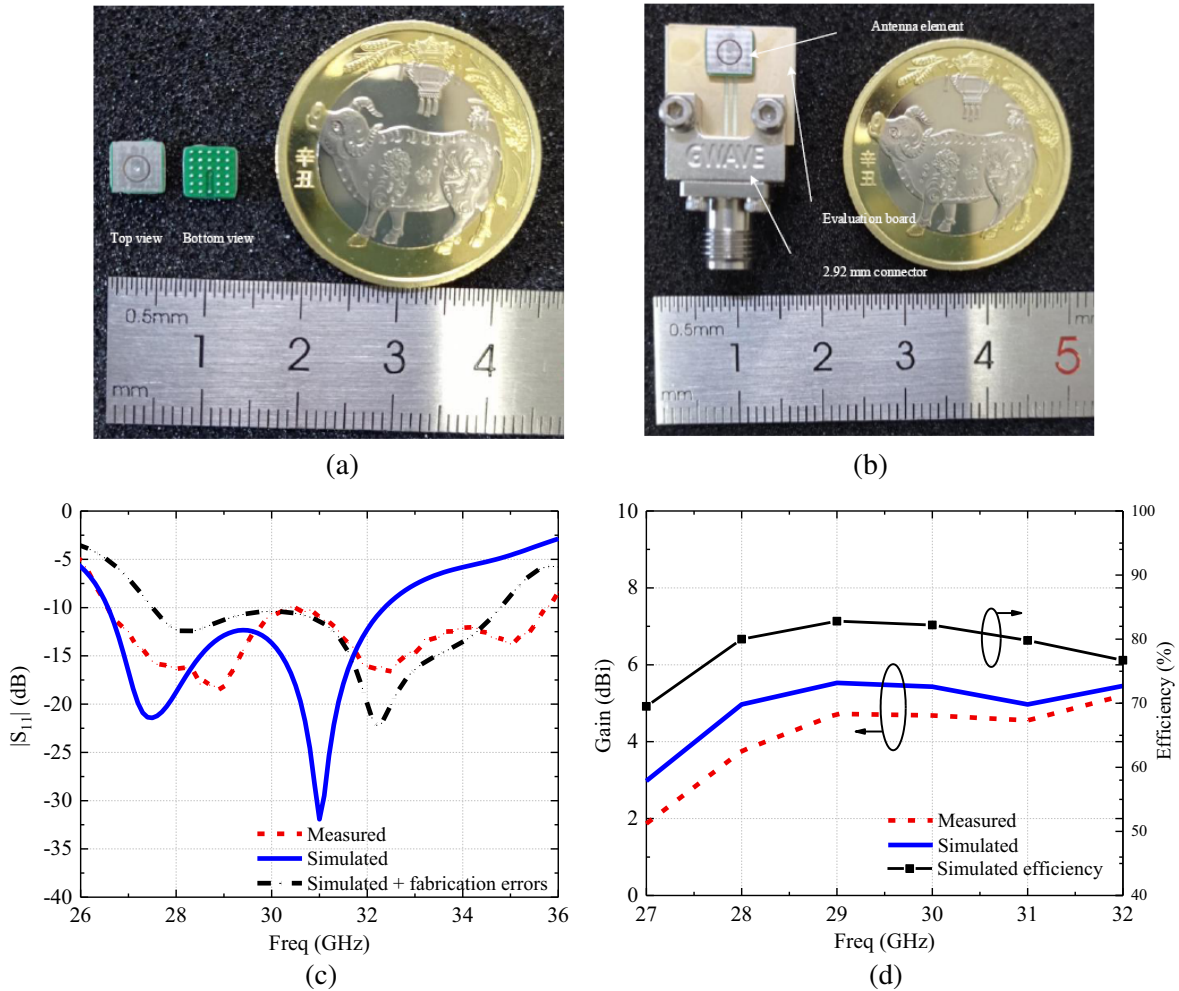


Figure 4. Photograph of the patch antenna prototype. (a) Antenna element. (b) Assembly prototype. (c) Measured and simulated reflection coefficient of the proposed antenna. (d) Measured and simulated peak gain of the proposed antenna.

PCB manufacturing. On the other hand, the permittivity usually varies with frequency. Therefore, we analyzed the influence of FR4 substrate size ($D1$) and permittivity on antenna performance. Figure 5(a) depicts the parameter analysis of the dielectric substrate size, and the permittivity analysis is shown in Figure 5(b). It can be seen that the smaller size ($D1$) will cause the resonance point to move to a higher frequency band and widen the operating bandwidth. Taking into account the prototype tolerance, we set $D1$ to 5.1 mm. Then we analyze the influence of the dielectric constant. It can be observed that a smaller permittivity will also cause the resonance point to move to a higher frequency and obtain a wider frequency band. As shown in Figure 4(c), the modified simulation results are in good agreement with the measured ones after considering the above manufacturing tolerances.

3.3. Comparison with Previous Works

Table 1 lists the main parameters of the proposed antenna and the reported antenna for comparison. The cost of the previously reported work [10] and [11] is relatively high. For example, LTCC is a high-cost material, and high-precision metal processing makes the manufacturing cost relatively high. In addition, the multi-layer configuration in [9, 15–17] also increases the cost. The work based on single-layer FR4 shows the advantage of ultra-low-cost. The application of the ring slot further reduces the size of the antenna, making it more compact and easier to integrate.

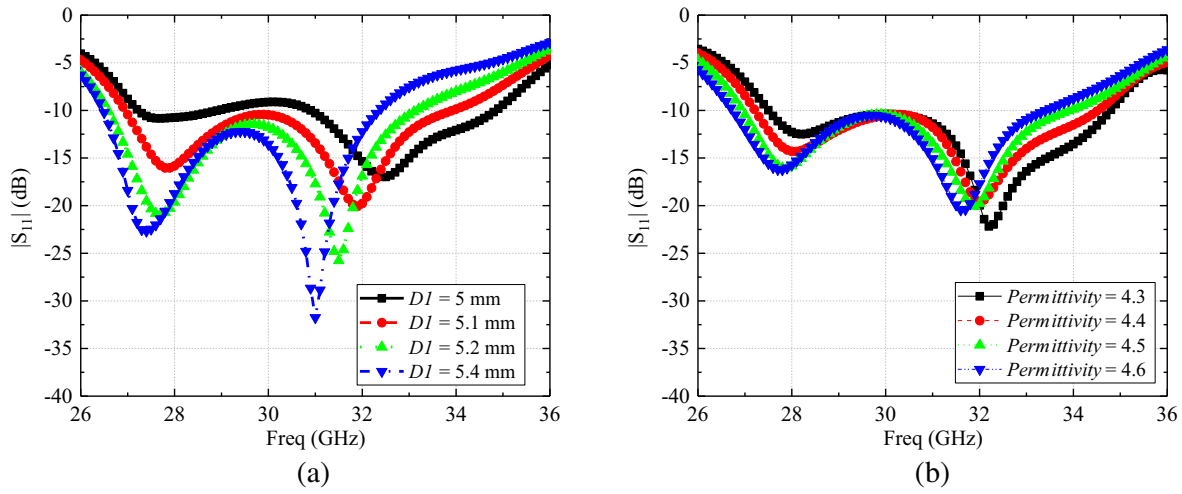


Figure 5. Simulated $|S_{11}|$ of the antenna element with different parameters. (a) $D1$. (b) Permittivity.

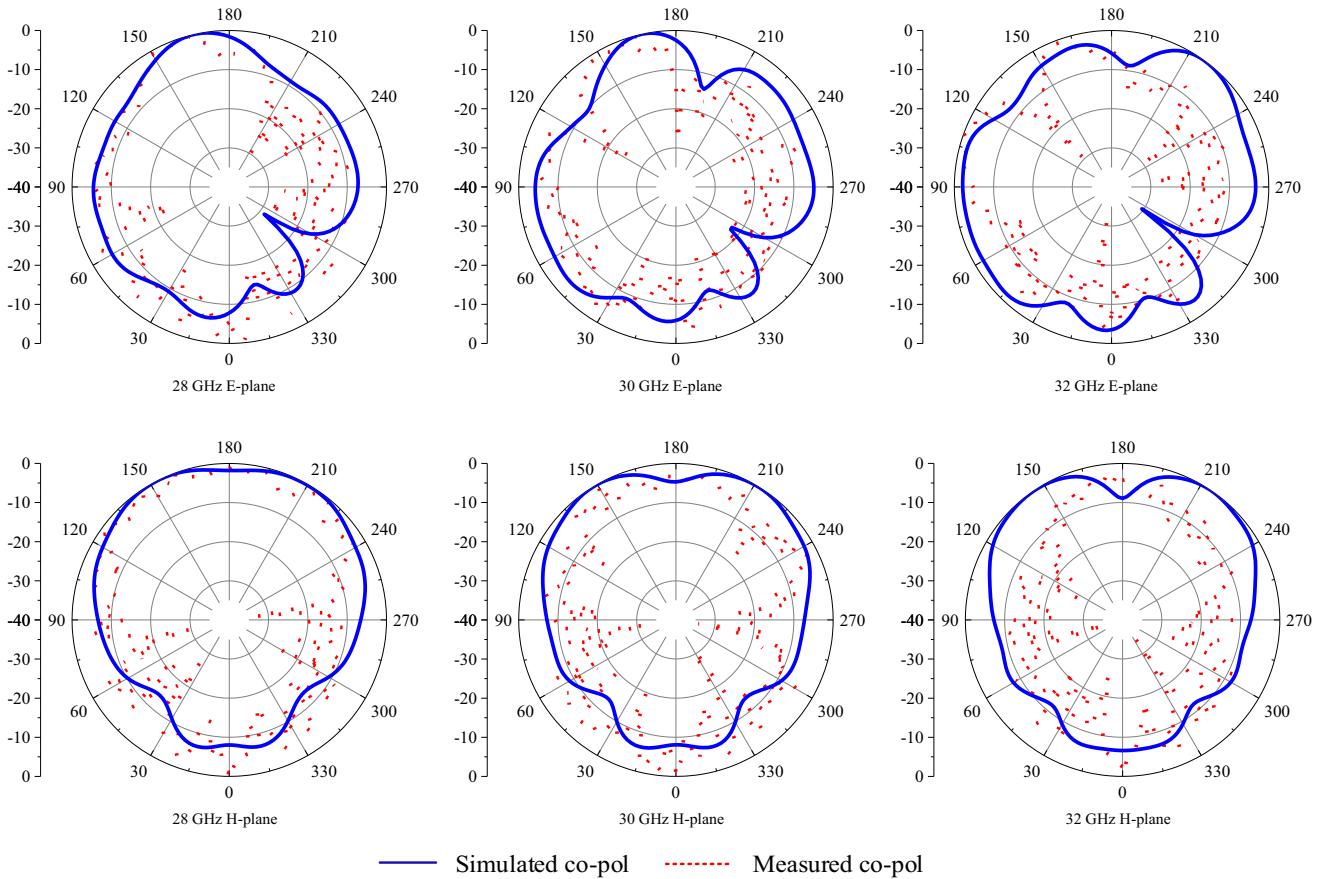


Figure 6. Simulated and measured E -plane (XOZ) and H -plane (YOZ) normalized radiation patterns at 28 GHz, 30 GHz and 32 GHz.

Due to the use of low-cost FR4 materials, the proposed antenna achieves cost-effective characteristics. At the same time, the BGA package enables the proposed solution to achieve a compact size, which makes it very suitable for integration into RF systems.

Table 1. Comparisons between the proposed and reported antennas.

Ref.	Antenna type	F_c	Imp. BW (-10 dB) (%)	Measured peak gain (dBi)	Dimensions of single element (mm ³)	Material
[9]	Patch	30.4	2.6%	4	6 × 6 *	Organic
[10]	PFSA	38	10.5%	2.43	5.4 × 1.8 × 0.89	LTCC
[11]	PIFA	28.62	2.4%	14.09 #	3 × 3.5 × 0.55	Stainless steel
[15]	Patch	27.8	14.4%	-	5 × 5 × 1.2	RO4003
[16]	Patch	26.875	26.8%	7.4	5.4 × 5.4 × 1.5	FR4&RO4350B
[17]	Patch	26	23.1%	11\$	6 × 6 × 1.2	FR4
[18]	PIFA	27.15	15.3%	5.85	4.5 × 4.5 × 1.3	FR4
[19]	Patch (U-slot)	33.45	15.2%	4.97	5 × 5 × 1.3	FR4
This work	Patch (Ring-slot)	31.15	29.2% &	5.2	5 × 5 × 1.3	FR4

* The thickness of the antenna element is not given.

Only 1 × 8 antenna array measured gain is given.

\$ Only 1 × 4 antenna array measured gain is given.

& -9.94 dB

4. CONCLUSIONS

This letter introduces a BGA packaged patch antenna with a ring slot. The antenna prototype has been successfully verified. By using an FR4 substrate, cost-effective functions can be obtained. With the introduction of BGA packaging, compact size and easy integration can be observed. The measurement results show that the -9.94 dB bandwidth of the antenna is 29.2%, which is in the range of 26.6–35.7 GHz. A peak gain of 5.2 dBi is obtained at 32 GHz. Experimental results show that the proposed antenna element can be used in the 5G mmWave frequency band (N257: 26.5–29.5 GHz, and N261: 27.5–28.35 GHz). The compact size and surface-mount function are attractive for integration into the 5G mmWave system.

ACKNOWLEDGMENT

The author would like to thank Prof Hongxing Zheng of the School of Electronics and Information Engineering, Hebei University of Technology, for helping with the antenna measurements.

REFERENCES

1. Carver, K. and J. Mink, "Microstrip antenna technology," *IEEE Trans. Antennas Propag.*, Vol. 29, No. 1, 2–24, Jan. 1981, doi: 10/dqgrtb.
2. Nasimuddin, X. Qing, and Z. N. Chen, "A wideband circularly polarized stacked slotted microstrip patch antenna," *IEEE Antennas Propag. Mag.*, Vol. 55, No. 6, 84–99, Dec. 2013, doi: 10/gjwzx6.
3. Telsang, T. M. and A. B. Kakade, "Ultrawideband slotted semicircular patch antenna," *Microw. Opt. Technol. Lett.*, Vol. 56, No. 2, 362–369, 2014, doi: 10/gj39ft.
4. Wang, H., X. B. Huang, and D. G. Fang, "A single layer wideband U-slot microstrip patch antenna array," *IEEE Antennas Wirel. Propag. Lett.*, Vol. 7, 9–12, 2008, doi: 10/d828rq.

5. Deshmukh, A. A. and K. P. Ray, "Compact broadband slotted rectangular microstrip antenna," *IEEE Antennas Wirel. Propag. Lett.*, Vol. 8, 1410–1413, 2009, doi: 10/ck8zkg.
6. Chair, R., C.-L. Mak, K.-F. Lee, K.-M. Luk, and A. A. Kishk, "Miniature wide-band half U-slot and half E-shaped patch antennas," *IEEE Trans. Antennas Propag.*, Vol. 53, No. 8, 2645–2652, Aug. 2005, doi: 10/cwf8p8.
7. Mitha, T. and M. Pour, "Conformal wideband microstrip patch antennas on cylindrical platforms," *Progress In Electromagnetics Research Letters*, Vol. 80, 1–6, 2018.
8. Zhang, Y. and J. Mao, "An overview of the development of antenna-in-package technology for highly integrated wireless devices," *Proc. IEEE*, Vol. 107, No. 11, 2265–2280, Nov. 2019, doi: 10.1109/JPROC.2019.2933267.
9. Liu, D., X. Gu, C. W. Baks, and A. Valdes-Garcia, "Antenna-in-package design considerations for Ka-band 5G communication applications," *IEEE Trans. Antennas Propag.*, Vol. 65, No. 12, 6372–6379, Dec. 2017, doi: 10.1109/TAP.2017.2722873.
10. Park, J., H. Seong, Y. N. Whang, and W. Hong, "Energy-efficient 5G phased arrays incorporating vertically polarized endfire planar folded slot antenna for mmWave mobile terminals," *IEEE Trans. Antennas Propag.*, Vol. 68, No. 1, 230–241, Jan. 2020, doi: 10/ghcvvw.
11. Park, J., D. Choi, and W. Hong, "Millimeter-wave phased-array antenna-in-package (AiP) using stamped metal process for enhanced heat dissipation," *IEEE Antennas Wirel. Propag. Lett.*, Vol. 18, No. 11, 2355–2359, Nov. 2019, doi: 10.1109/LAWP.2019.2938229.
12. Zhang, Y. P., "Integration of microstrip patch antenna on ceramic ball grid array package," *Electron. Lett.*, Vol. 38, No. 5, 207–208, Feb. 2002, doi: 10.1049/el:20020144.
13. Zhang, Y. P., "Integrated circuit ceramic ball grid array package antenna," *IEEE Trans. Antennas Propag.*, Vol. 52, No. 10, 2538–2544, Oct. 2004, doi: 10.1109/TAP.2004.834427.
14. Sun, M., Y. P. Zhang, Y. X. Guo, K. M. Chua, and L. L. Wai, "Integration of grid array antenna in chip package for highly integrated 60-GHz radios," *IEEE Antennas Wirel. Propag. Lett.*, Vol. 8, 1364–1366, 2009, doi: 10.1109/LAWP.2009.2039031.
15. SalarRahimi, M., et al., "A cost-efficient 28 GHz integrated antenna array with full impedance matrix characterization for 5G NR," *IEEE Antennas Wirel. Propag. Lett.*, Vol. 19, No. 4, 666–670, Apr. 2020, doi: 10/ghh7w4.
16. Lima de Paula, I., et al., "Cost-effective high-performance air-filled siw antenna array for the global 5G 26 GHz and 28 GHz bands," *IEEE Antennas Wirel. Propag. Lett.*, Vol. 20, No. 2, 194–198, Feb. 2021, doi: 10/gjxczb.
17. Kim, G. and S. Kim, "Design and analysis of dual polarized broadband microstrip patch antenna for 5G mmWave antenna module on FR4 substrate," *IEEE Access*, Vol. 9, 64306–64316, 2021, doi: 10/gjxzh2.
18. Wang, X., X. Liu, W. Zhang, D. Hao, and Y. Liu, "Surface-mount PIFA using ball grid array packaging for 5G mmWave," *Progress In Electromagnetics Research Letters*, Vol. 98, 55–60, 2021.
19. Wang, X., X. Liu, W. Zhang, D. Hao, and Y. Liu, "Surface mounted microstrip antenna using ball grid array packaging for mmWave systems integration," *Progress In Electromagnetics Research Letters*, Vol. 98, 105–111, 2021.